Journal of Applied Polymer Science

Compatibility Study of Chlorinated Polyethylene/Ethylene Methacrylate Copolymer Blends Using Thermal, Mechanical, and Chemical Analysis

Purabi Bhagabati, T. K. Chaki
Rubber Technology Centre, Indian Institute of Technology Kharagpur, Kharagpur 721302, West Bengal, India
Correspondence to: T. K. Chaki (E-mail: tapanchaki2009@gmail.com)

ABSTRACT: Blends of chlorinated polyethylene (CPE) elastomer and ethylene methacrylate copolymer (EMA) in various compositions were studied for their compatibility using differential scanning calorimetry (DSC), dynamic mechanical analysis (DMA), and Fourier transform infrared (FTIR) spectroscopy techniques. Irrespective of measurement techniques used, all blends showed a single glass transition temperature (T_g) lying in between the T_g of control polymers in both DSC and DMA. Glass transition temperatures of blends obtained from DSC were in consistency with Couchman–Karasz equation. Also, the T_g obtained from both DSC and DMA are above the "rule of mixing" line of the two control polymers. These results from thermal analysis clearly indicate some compatibility between the two polymers. Furthermore, compatibility of CPE/EMA blends were also been investigated by FTIR spectroscopy and scanning electron microscopic analysis. A shifting of characteristic C—Cl stretching peak of CPE and C=O stretching peak of EMA toward lower wave number indicate the presence of specific interaction between the two polymers. Mechanical properties like tensile strength, modulus at 100% elongation, elongation at break, and hardness were observed above the line of additivity drawn between the two control polymers, which corroborate compatibility between CPE and EMA. © 2013 Wiley Periodicals, Inc. J. Appl. Polym. Sci. **2014**, *131*, 40316.

KEYWORDS: blends; compatibilization; differential scanning calorimetry (DSC); copolymers; elastomers

Received 17 October 2013; accepted 17 December 2013
DOI: 10.1002/app.40316

INTRODUCTION

Blending of rubbers is one of the most widely adopted technique in product development area of rubber industry due to the reason that developing a solely new material with required criteria is really a tough and tedious job, which needs not only long time but also consumes huge effort and economy. On the contrary, effective blending of two or more rubber with desired set of performance characteristics can allow the new product to get into a special application field where the constituent single rubber material alone cannot enter. Miscible blends are homogeneous and exist as single phase polymer while technologically compatible blends are inhomogeneous and show phase separated morphology with appreciable level of intermolecular interaction between phases. From the past few decades, numerous rubber blends of type miscible, compatible, or polymer alloy with modified morphology have been developed and successfully commercialized. Most of the industrially successful rubber blends are either miscible or well compatible with each other and hence their properties mainly depend on the properties of pure rubber. On the other hand, properties of incompatible blends are not only dependent on base rubbers but also dependent on their blend morphology like interfacial adhesion, dispersed domain size, type of dispersion, etc. Homogeneity of rubber blends at a microscopic level is very much necessary to get optimum performance. But often rubber technologists prefer to have certain degree of microheterogeneity in order to uphold the individual performance properties of the respective rubber components.[1] Hence, technological compatibility of rubber blend is of utmost important factor in industrial application for efficient property control.[2] When the interfacial adhesion between the rubber components are reasonably high, their morphological heterogeneity is sufficiently small (<100 Å) and in such cases the heterogeneity of ostensibly homogeneous blend is unobservable by many experiments like differential scanning calorimetry (DSC), dynamic mechanical analysis (DMA) which shows only one composition dependent glass transition temperature (T_g).[3] In contrast Fourier transform infrared (FTIR) spectroscopy is one of the most promising technique to qualitatively reveal the existence of any specific interaction between the constituent polymers of miscible or compatible blends.[4,5] Chlorinated polyethylene (CPE) is a special class of elastomer which is prepared from polyethylene by random chlorination in aqueous medium and therefore, it is always available in the form of powder. It possesses numerous advantageous properties over

other unsaturated and saturated elastomers. The saturated backbone of CPE imparts excellent weather resistance, ozone resistance, oxidation resistance, chemical resistance, hydrocarbon oil resistance, very good compression set property, low temperature flexibility, heat aging resistance, and very good processability. Moreover, the presence of chlorine atom in the backbone of CPE gives inherent flame retardancy.[6] Besides these special performance advantages, CPE can give cost advantages over many other elastomers like chlorosulphonated polyethylene (CSPE), chloroprene rubber (CR), ethylene vinyl acetate copolymer (EVA), ethylene methacrylate copolymer (EMA), and many other saturated and unsaturated elastomers. Blending of CPE with other polymers has drawn lot of attention of researchers and polymer technologists. A lot of study has been done where CPE is blended with natural rubber (NR), polyurethane (PU), polyvinyl chloride (PVC), acrylonitrile butadiene rubber (NBR), and many other polymers for its improved properties in accordance with service requirement.[7–10] Likewise CPE, the EMA also has saturated backbone due to which it has very good age, oil and thermal degradation resistance property. Also it has excellent low temperature flexibility which is much better than CPE even without any plasticizer. Both the CPE and EMA are widely used in market in industries especially for wire and cable covering. Although halogen containing polymers have fire retardant capacity, but many a time manufacturer of wire and cable shows their concern about the secondary effect of fire which causes much severe damage to other systems and environment compared with the cable. All halogen containing polymers produce toxic and corrosive gases once it gets fire. So blending of EMA with CPE would reduce the adverse effect of halogen in the polymer used for wire and cable cover and jacketing. Blending of EMA with CPE could not only retain age, oil and thermal degradation resistance but can also render low temperature flexibility of EMA and cost advantage of CPE. In this article, a thorough study was made on compatibility of CPE and EMA in various blend compositions with the help of DSC, DMA, and FTIR tools. Mechanical properties and morphology for all blend compositions were also been discussed in order to find the effect of compatibility.

EXPERIMENTAL

Materials

Commercial grade CPE rubber (CPE 360) with 36% Cl content, having density of 1.213 g cm^{-3} with Mooney viscosity $ML_{(1+4)}$ at 121°C of 65 ± 5 was obtained from East Corp International, India. Commercial grade of EMA, Elvaloy® 1330 with 30% methyl acrylate (MA) content and a melt flow index (MFI) (at 190°C/2.16 kg) of 3.0 g 10 min^{-1} (ASTM D1238) having melting point of 85°C was obtained from NICCO Corporation, Shyamnagar, India. Magnesium oxide (MgO) of density 3.58 g cm^{-3} was used as acid scavenger for hydrochloric acid (HCl) produced during processing and molding. Dibutyltin dilaurate (DBTDL) and Irganox 1010 which were procured from Sigma-Aldrich were used as heat stabilizer of CPE and as antioxidant, respectively.

Table I. Sample Designations with Composition Along with their Experimental Glass Transition Temperature (T_g) from DSC Analysis

Sample designations	CPE	EMA	Glass transition temperature (T_g) (experimental)
C100E0	100	0	−12.0
C80E20	80	20	−14.2
C60E40	60	40	−17.1
C50E50	50	50	−18.6
C40E60	40	60	−20.0
C20E80	20	80	−23.6
C0E100	0	100	−31.0

Method of Blend Preparation

CPE, EMA, and all other ingredients were mixed in HAAKE Rheomix OS (Germany) 600 internal mixer, having a mixing chamber volume 67 cm^3 at a rotor speed of 60 rpm at 140°C for 8 min. CPE was first softened for 2 min along with MgO, DBTDL, and Irganox 1010; which was followed by addition of EMA. Then the mixing was continued six more minutes. The mixes so obtained were sheeted out in a two roll mill with nip gap of 2 mm. The sheets were compression molded into 2 mm thick slabs in an electrically heated hydraulic press (Moore Presses, George E. Moore & Sons Birmingham, UK) at 120°C under a pressure of 10 MPa for 4 min. The mold was allowed to cool under the same pressure to room temperature before removing the slab from mold. The designations of all the blend samples are given in Table I. MgO, Irganox 1010, and DBTDL are kept constant in all samples with the amount of 3 phr, 1 phr, and 1 phr, respectively.

Characterization of Blends

DSC. DSC measurements were carried out using a TA instrument (Model DSC Q100 V 8.1) to study the phase transformation and heat capacity values of polymer blends and its control samples. All samples of about 6 mg was sealed in aluminum pans and were heated from −70°C to +150°C at a heating rate of 10°C min^{-1} under nitrogen atmosphere. All glass transition temperatures (T_g) and melting behavior were observed from second heating run of DSC plot.

DMA. The dynamic mechanical properties of the blends were studied by using a DMA of TA instruments (model Q800). All samples (12.59 mm × 6.65 mm × 1.2 mm) were cut from compression molded sheets. Tests were carried out in the tensile mode at a constant frequency of 1 Hz, a strain of 0.05% and a temperature range from −100°C to 150°C at a heating rate of 3°C min^{-1}. The data were analyzed by TA Universal analysis software on a TA computer attached to the machine. Storage modulus (E′) and loss tangent (tan δ) were obtained as a function of temperature for all the samples under identical test conditions. The temperature corresponding to the peak in tan δ versus temperature plot was taken as the T_g.

FTIR Analysis. The FTIR spectra of control polymer and their blends (CPE/EMA) were recorded in a FTIR spectrometer

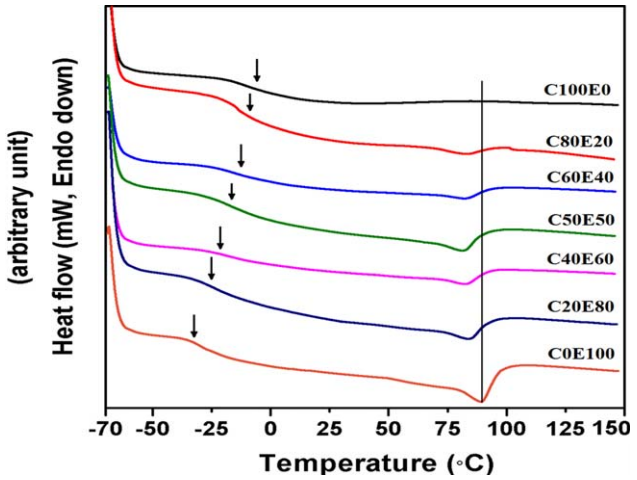

Figure 1. Normalized DSC thermograms for control CPE, control EMA, and their blends with different compositions. [Color figure can be viewed in the online issue, which is available at wileyonlinelibrary.com.]

Bruker Equinox 55 in ATR mode in the region of 4000–600 cm^{-1} and 32 scans were collected with a spectral resolution of 0.5 cm^{-1}. An average of three scans for each sample was taken for the measurement.

Mechanical Property. Tensile specimens ASTM D 412-98 were punched from the molded sheets using ASTM Die-C. Tensile strength, modulus, and percent elongation at break of all samples were measured according to ASTM D418-98A using a universal testing machine (UTM) Hounsfield H10KS (UK) at a constant cross-head speed of 500 mm min^{-1}. All results reported were based on the average values of result of five samples and the standard deviations of these values are indicated by the relevant line segments. The error in the measurement for tensile strength was ±1%, ±0.5% for modulus at 100% elongation, and ±3% for elongation at break. Hardness was reported in Shore A scale measured in Rex Durometers (as per ASTM D2240 method) Model 2000, Buffalo Grove.

Morphological Study

Morphological studies of few particular blends were carried out using a scanning electron microscope (SEM), (model ZEISS EVO 60, Carl ZEISS SMT, Germany), operating at 20 kV. For this, the cryogenically smoothened surface of the sheeted blends was etched by a suitable solvent (chloroform) to selectively extract only the EMA phase. The extraction process was carried out at 50°C for 1 hr. The samples were then dried in vacuum oven at 50°C for 12 hr to remove the solvent. The dried samples were coated with gold and subsequently examined their morphology.

RESULT AND DISCUSSION

DSC

Among different characterization techniques, DSC is one of the potential method to determine miscibility of polymer blends. It is well established that any two polymers are compatible with each other if they show a single T_g, intermediate between the two control polymers. The DSC graph in second heating run of all blends with different compositions along with the control polymers are shown in Figure 1 from which T_g and melting behaviors (T_m) can be observed. It reveals that all blends show only single T_g positioned in between the T_g of the control polymers. Hence, the prepared blends are compatible in all proportions. The obtained experimental T_g values of the compatible blends along with the control polymers are enlisted in Table I. In our study, control EMA shows T_g at −31°C and control CPE shows a T_g at −12°C and these values are close to the literature values.[11,12] Generally, when there is an interaction between the constituent polymers in blend, then the T_g value increases due to the development of restriction in molecular motion of polymer chains. Therefore, the T_g values show a positive deviation from the Rule of mixing.[13] Although the difference between the T_g obtained from the DSC instrument of control polymers are not high, but discussion on model fitting of experimental T_g values and its clear positive deviation from Rule of mixing as shown in the succeeding section endorses the concept of compatibility.

To substantiate the above acclaimed point on compatibility between CPE/EMA, melting behavior of all blends as well as control polymer samples were discussed. A small and broad crystalline melting peak of control EMA is observed at around 85°C and the broadness of this peak is probably due to presence of large number of small crystallites in the EMA.[14] In a polymer blend when one component is crystallizable and the other is not; as explained by Nishi and Wang, a melting point depression of the crystalline phase provide an additional evidence of miscibility.[15,16] The similar phenomenon of depression of melting point of semicrystalline EMA on addition of purely amorphous rubber CPE is observed in Figure 1, which assesses the compatibility of the CPE/EMA blend system.

Model Fitting. There are many models available in the literature to predict the glass transition temperature of polymer blends with different level of crystallinity of pure polymers.[17] The composition dependency of T_g obtained from DSC analysis of CPE/EMA blends are shown in Figure 2. Here the reason for positive deviation in T_g values of all blends from the linearity, as often

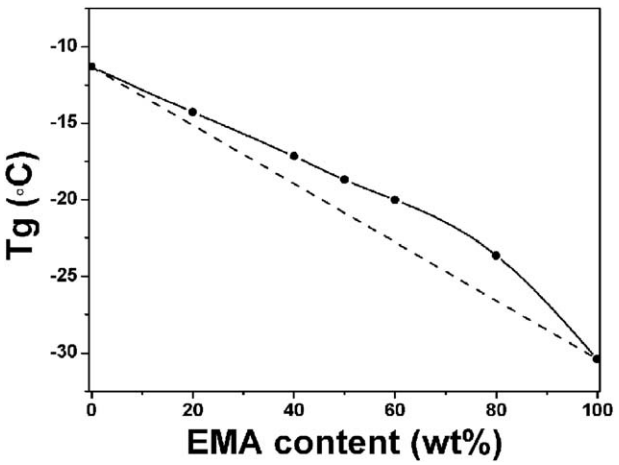

Figure 2. Comparison of T_g obtained from DSC of blends with Rule of mixing. *Solid line* represents experimental values and *dashed line* represents mixing rule.

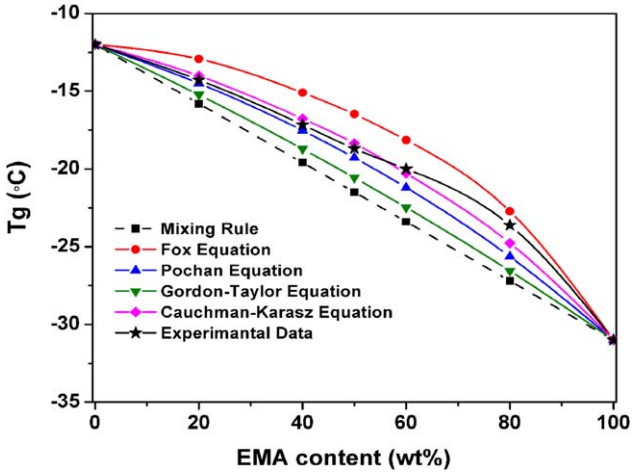

Figure 3. Plots of theoretically calculated T_g of CPE/EMA blends as a function of EMA content in accordance to different proposed equations along with the experimental T_g values of DSC. [Color figure can be viewed in the online issue, which is available at wileyonlinelibrary.com.]

observed for miscible blends, could be ascribed to specific interactions between segments of both polymers.[18,19] The details of interaction between the two polymers are discussed later by using FTIR tool.

The more general equation for composition dependent T_g in a binary mixture was proposed by Couchman and Karasz of eq. (1).[20,21] In this equation, it is assumed that ΔC_{pi} is independent of temperature. The equation is mentioned below:

$$\ln T_g = \frac{W_1 \times \Delta C_{p1} \times \ln T_{g1} + W_2 \times \Delta C_{p2} \times \ln T_{g2}}{W_1 \times \Delta C_{p1} + W_2 \times \Delta C_{p2}} \quad (1)$$

T_g is the glass transition temperature of the blend, W_i is the weight fraction of component i, and ΔC_{pi} is the difference in specific heat between the liquid and glassy states at T_{gi}.

As proposed by Pochan et al., in the eq. (1) if ΔC_{p1} (the polymer with lower T_g) and ΔC_{p2} are assumed to be almost of same value, that is, $\Delta C_{p1} = \Delta C_{p2}$, then we will get eq. (2) as mentioned below.[22]

$$\ln T_g = W_1 \times \ln T_{g1} + W_2 \times \ln T_{g2} \quad (2)$$

Assuming again that $\Delta C_{p1} = \Delta C_{p2}$, after rearrangement and expansion of eq. (2), the Fox equation can be obtained in eq. (3) as given below:

$$\frac{1}{T_g} = \frac{W_1}{T_{g1}} + \frac{W_2}{T_{g2}} \quad (3)$$

The eq. (1) can directly be derived to Gordon–Taylor equation with the condition that T_{g2}/T_{g1} is close to unity and considering $k = \Delta C_{p1}/\Delta C_{p2}$, and hence the eq. (4) will be as follows.[23,24]

$$\ln T_g = \frac{W_1 \times T_{g1} + k \times W_2 \times T_{g2}}{W_1 + k \times W_2} \quad (4)$$

The Fox equation [eq. (3)] assumes random mixing of the two polymers in the blend, with equal values of ΔC_{pi} at their glass transition temperatures, and no volume expansion between the two polymers during mixing. In such case the two polymers are completely miscible with each other. Since in our study, the experimental T_gs of all blends do not fit with Fox equation as evident from Figure 3, therefore in this case the heat capacity of the two polymers should be considered.[25] The ΔC_p value of EMA and CPE is found to be 0.355 J g^{-1} K^{-1} and 0.290 J g^{-1} K^{-1}, respectively. Also here the T_g values of control polymers differ from each other and hence T_{g2}/T_{g1} does not tend to unity. Therefore, here it is best to consider the Cauchman and Karasz equation [eq. (1)], although eqs. (2), (3), and (4) curves have also been plotted in Figure 3. The experimental T_g of all blends versus composition curve closely fits to the predicted Couchman–Karasz equation, while curve for Pochan equation also goes close but not to the blends with higher EMA content. As mentioned above, the experimental T_g of all CPE/EMA blends do not fit well with Fox equation and therefore it is not a completely miscible blend unlike random copolymers. But the T_g of all blends are showing a clear positive deviation from rule of mixing and this result suggests that the studied blend systems are compatible in all composition.

DMA Studies

In order to verify the presence of single T_g of CPE/EMA blends as obtained from DSC results, a temperature sweep experiment of DMA was also been carried out within the temperature range of −100°C to 150°C for all blends and control polymers. A miscible or a technologically compatible blend shows only one peak corresponding to T_g in temperature sweep plot of loss modulus which should be positioned in between the two control polymers. The tan δ versus temperature plot of all blend compositions along with their control systems are shown in Figure 4. In this plot, control EMA shows one major peak at −15°C which is the β_c-relaxation corresponding to crystal constrained glass-rubber relaxation.[26] Another tiny peak associates this glass rubber transition peak at around 31°C and this is called α-relaxation peak. This α-relaxation peak is related to onset of molecular motion in the crystalline phase and hence appears as a small peak.[27] On the other hand, control CPE shows glass transition temperature at around 10°C which is almost close to the value reported by Sirisinha et al.[28] Similar

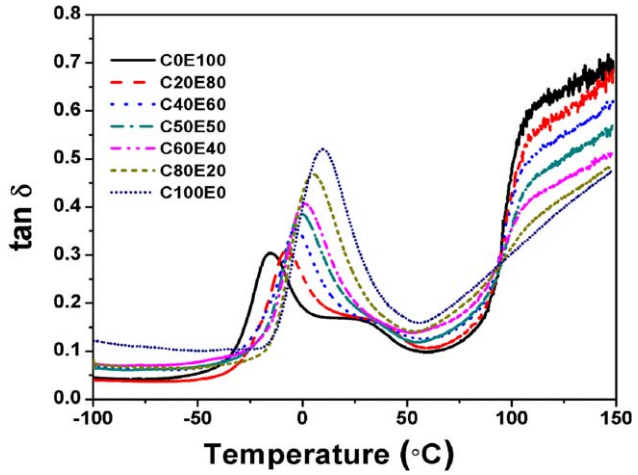

Figure 4. The tan δ versus temperature plot of control CPE, EMA, and their blends indicating T_g. [Color figure can be viewed in the online issue, which is available at wileyonlinelibrary.com.]

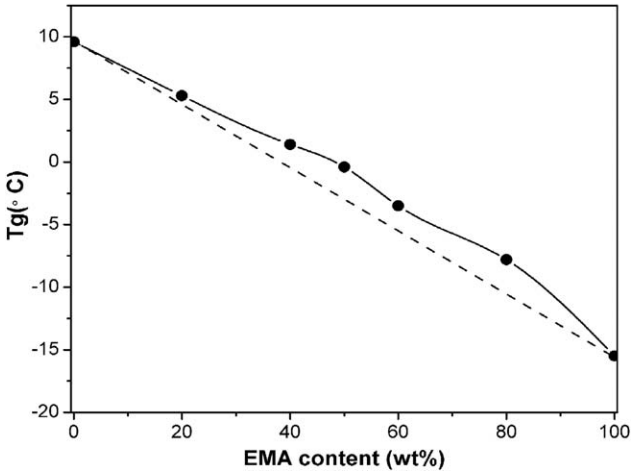

Figure 5. Variation of T_g obtained from DMA results with blends composition and a comparison with mixing rule.

with DSC data (where only one inflection for T_g is observed), DMA also displays only one major peak in loss tangent versus temperature plot which corresponds to glass–rubber transition of all blends. In addition to this, T_g of all blends obtained from DMA results also shows positive deviation from "Rule of mixing" as depicted in Figure 5. This clearly indicates some miscibility or technological compatibility between the two polymers in all blend compositions.

Another standpoint involves shifting of the β_c glass–rubber relaxation peak of semicrystalline EMA from −15°C to higher temperature in blends. Also the α-transition peak is observable only in case of blends C20E80 and C40E60 including control EMA, which is due to dilution effect of amorphous CPE. It is interesting to observe that the α-transition peak of EMA is also shifting to higher temperature on adding CPE to EMA. Increasing CPE content in the blend is leading appreciable shifting of the transition peak to even higher temperature. This shifting of peaks is attributed to specific interaction between EMA and CPE as further convinced by FTIR data, which results restriction

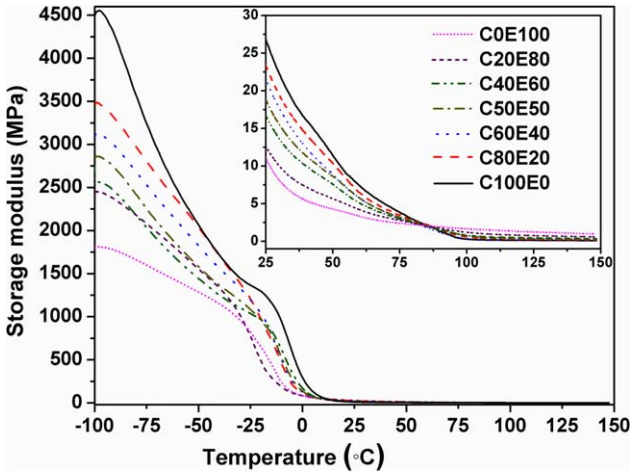

Figure 6. Storage modulus (E') versus temperature plot for CPE, EMA, and their different blends. [Color figure can be viewed in the online issue, which is available at wileyonlinelibrary.com.]

Table II. Storage Modulus of Control Polymers and Their Blends with Different Composition at 75°C and at 100°C

Samples	Storage modulus (MPa) at 75°C	Storage modulus (MPa) at 100°C
C100E0	2.39	1.67
C80E20	2.78	1.21
C60E40	2.96	0.84
C50E50	3.22	0.76
C40E60	3.47	0.59
C20E80	3.64	0.32
C0E100	3.87	0.28

of motion of side chain ester group and restriction of the onset of molecular motion in the crystalline phase.[27] Moreover, CPE and EMA have similar backbone structure (polyethylene segment in the main chain) and because of such structural similarity, some partial miscibility between the two polymers in their amorphous region exists.

In the E′ versus temperature plot in Figure 6, control CPE shows highest storage modulus at low temperature followed by a steep fall in E′ values at its transition region which is due to the reason of amorphous nature of CPE. Addition of EMA to CPE brings down the E′ value at low temperature and at its transition region the value shows rather a gradual decrease which is due to the presence of crystalline part of EMA. Since during the glass transition of semicrystalline material, only the amorphous part undergoes segmental motion, whereas the crystalline part remains crystalline solid until reaching the temperature of melting.[29] Hence, it is seen that as the EMA content in blend increases, the sharpness in fall of storage modulus at the transition region decreases. The storage modulus after the transition, that is, E′ at high temperature increases with increasing EMA content and control EMA has the highest rigidity above the transition which is again due to the influence of the crystalline region of EMA.[30] Higher E′ value above the transition indicates higher ability of the material to withstand distortion. One interesting result observed in Figure 6 is that, up to a high temperature of about 75°C, the blends with higher EMA content shows higher storage modulus, but at temperature around 85°C, a crossover is seen. After this crossover as temperature increased, the storage modulus of higher EMA containing blends show lower value and this trend remains same up to the experimental temperature range of 150°C. This is because of the semicrystalline nature of EMA and at around 85°C, all the crystallite of EMA melts and as a result modulus also decreased. Hence at higher temperature above 85°C onward, EMA rich blends show lower E′ value. Storage modulus of control polymers along with their blends before crossover point at 75°C and after the crossover point at 100°C is tabulated in Table II.

FTIR Studies

The FTIR spectra of CPE, EMA, and their blends give evidence for the interaction between the two polymers as shown in Figure 7. The characteristic peaks of CPE with random chlorination between 25% and 47% are expected to be similar with

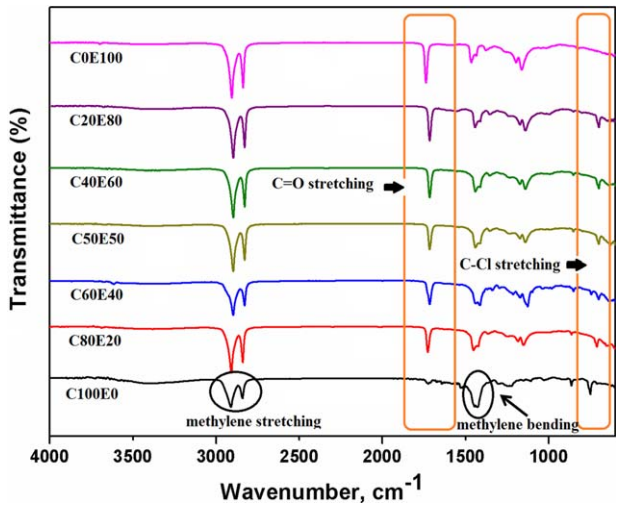

Figure 7. FTIR spectra of control CPE, EMA, and their blends. [Color figure can be viewed in the online issue, which is available at wileyonlinelibrary.com.]

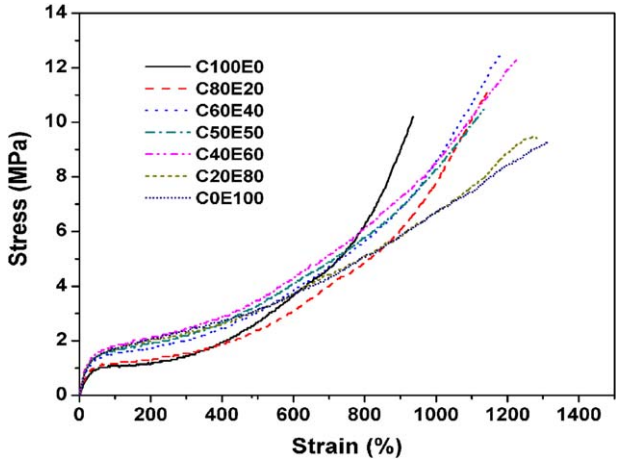

Figure 9. Stress–strain diagram of control CPE, EMA, and their blends. [Color figure can be viewed in the online issue, which is available at wileyonlinelibrary.com.]

PVC, possibly stronger C—H stretches and bends; and weaker C—Cl stretches.[31] The peaks at 2916 and 2850 cm^{-1} are observed which corresponds to methylene stretching. Also a methylene bending peak is observed at around 1448 cm^{-1}. A weak stretching peak for C—Cl is observed at 709 cm^{-1} for control CPE. The methine C—H stretch peak which should be at around 2900 cm^{-1} is been overlapped or buried by methylene stretching peak observed at 2916 and 2850 cm^{-1}.

A sharp peak of carbonyl (C═O) stretching is observed for control EMA at 1736 cm^{-1} which is shifting to 1730 cm^{-1} in all blends. Fekete et al. and Aouachria et al. reported the existence of specific interaction of hydrogen bond type between the carbonyl (C═O) of acrylate group of PMMA and hydrogen atom of CHCl group in PVC.[32,33] Coleman et al. suggested a perfect possibility of presence of a specific interaction of hydrogen bonding type (—C═O·····H—C—Cl) between the carbonyl C═O of EVA and methine H atom of CPE. The C—Cl stretching vibrations occur in the region of 600–750 cm^{-1} and in our study, the typical C—Cl stretching peak for base CPE is observed at 709 cm^{-1} and it lowers to around 700 cm^{-1} in CPE/EMA blends. The shifting of C—Cl stretching peak could also be interpreted on the ground of hydrogen bond type interaction between C═O of EMA and methine hydrogen of CPE,

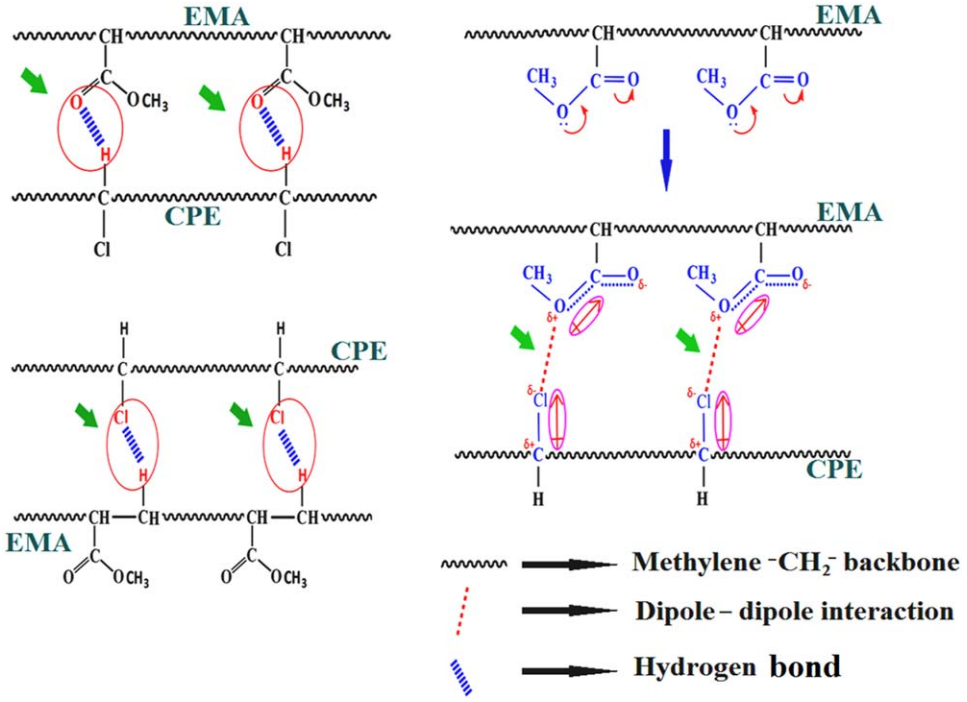

Figure 8. Diagram of plausible interaction between CPE and EMA based on FTIR spectra. [Color figure can be viewed in the online issue, which is available at wileyonlinelibrary.com.]

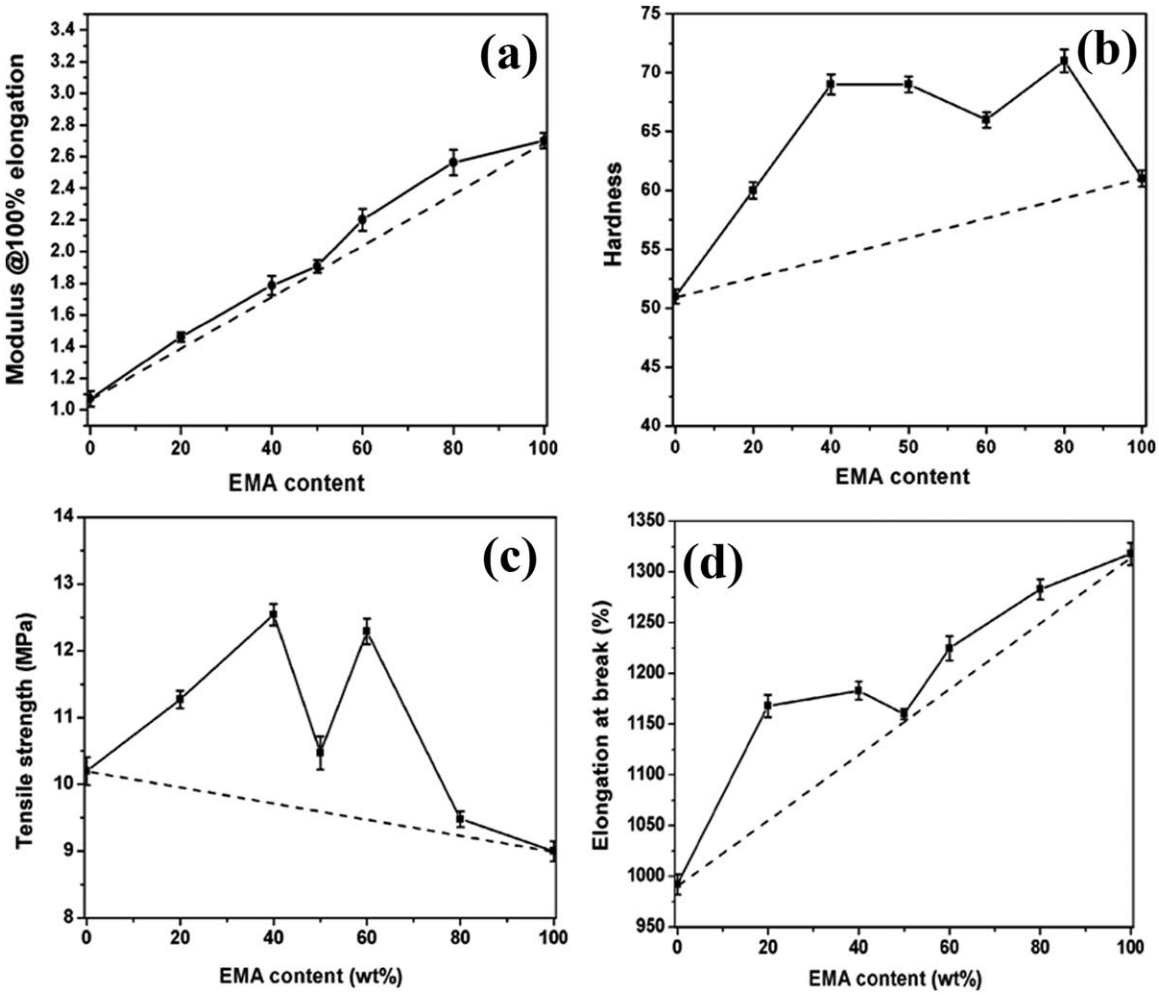

Figure 10. Figures showing variation of (**a**) modulus at 100% elongation at break, (**b**) shore A hardness, (**c**) tensile strength, and (**d**) elongation at break of different blend compositions along with their control systems. (The *solid lines* represent the experimental values and *dashed line* represents the additivity line drawn between control polymers).

which would result changes in the C—Cl stretching frequency without its direct involvement in any interaction.[34] However, another possibility for C—Cl stretching peak shifting could be attributed to a feeble interaction between C—Cl dipole of CPE and the β-hydrogen of acrylate ester of EMA.[35] Nevertheless, the possibility for dipole–dipole interaction between the polar groups of the two polymers cannot be ruled out.[26] Based on the above discussion, various plausible interactions between CPE and EMA are shown in Figure 8. In this figure, all hydrogen bond and dipole–dipole interactions are encircled and indicated with an arrow mark for elucidation.

Mechanical Properties of Blend

Mechanical properties of the two polymers and their blends were determined which also help correlating it with compatibility between the two polymers in blends. In Figure 9, the stress–strain diagram of all blends of different compositions along with their control systems are shown. It can be observed clearly from the Figure 9 that control CPE graph is showing steep rise after 700% elongation which could be because of strain induced crystallization of amorphous CPE. Similarly, blends with higher weight percent of CPE is showing steep rise in stress–strain plot after a certain percent elongation. Hence all systems other than control EMA and C20E80 are showing almost similar stress–strain behavior. It is also clear from the diagram that with increasing EMA content the initial modulus increased. The variation of modulus at 100%, shore A hardness, tensile strength, and elongation at break, with different weight percent of EMA including control polymers are shown in Figure 10. Modulus at 100% and hardness of pure EMA is higher than pure CPE. The reason for this is because of amorphous nature of CPE rubber, whereas EMA is a semicrystalline polymer.[14] When a comparatively more crystalline polymer is added to purely amorphous polymer like rubbers, then the mechanical property measured under no strain (e.g., hardness) and under low strain (e.g., modulus at 100% elongation) show a synergism. This synergism is because of the increase in crystallinity due to the presence of more crystalline component and here compatibility does not play a significant role.[36] On the other hand, tensile strength and elongation at break are the mechanical properties which are determined at high strain level. Only blends with good compatibility can show synergistic behavior in high strain mechanical

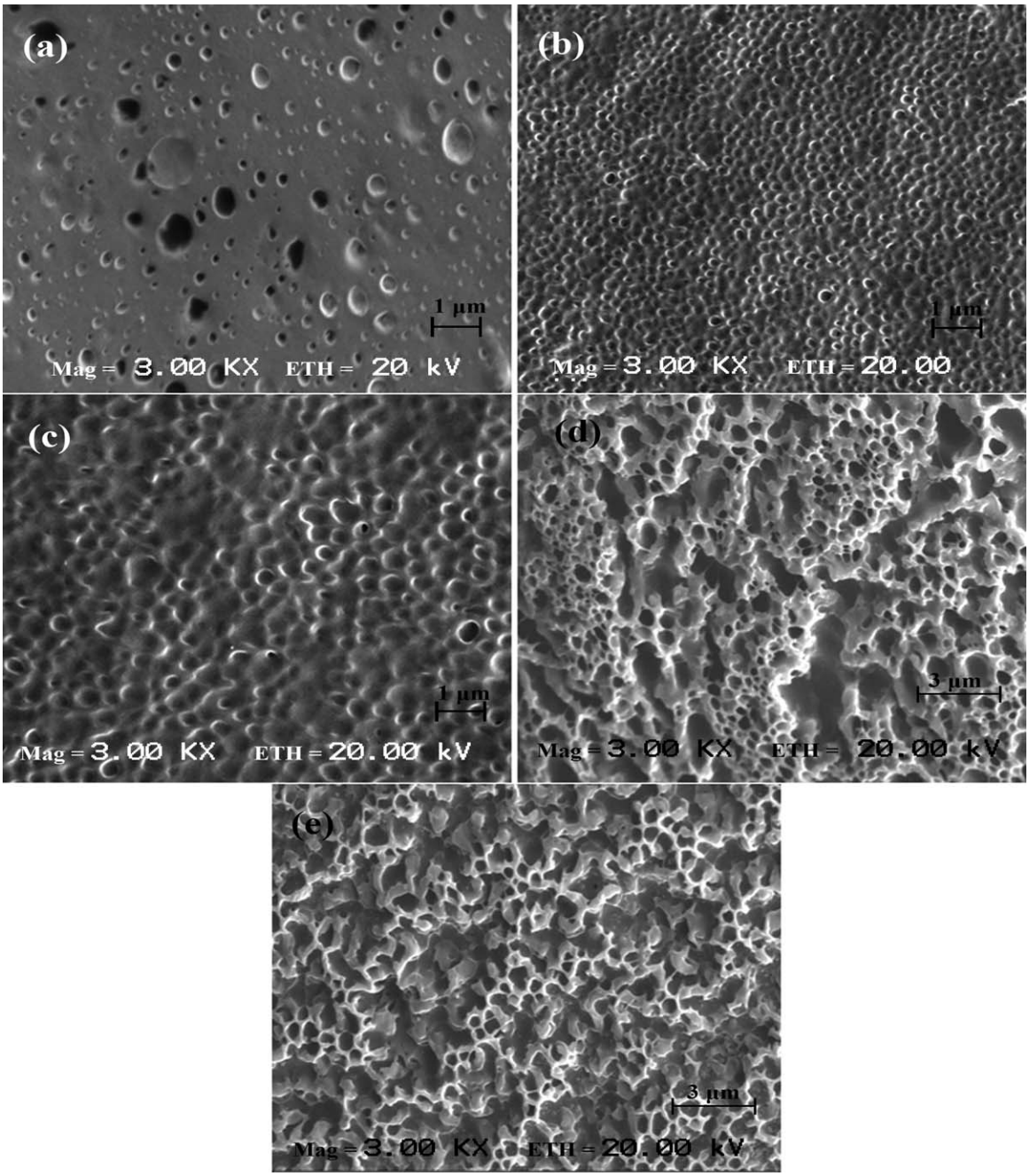

Figure 11. Scanning electron micrographs of cryogenically smoothened CPE, EMA, and their blends.

properties. There is potential influence of interfacial interaction between phases of polymers in any polymer blends. It is quite obvious that, blends with high interfacial tension like PE/PS follow a negative deviation in mechanical behavior from mixing rule. Polymer blends with good specific interaction might not be completely miscible to each other but they will be technologically compatible. For technologically compatible blends, the mechanical property variation can potentially be influenced by the degree of compatibility. Higher the technological compatibility of polymers in blend, higher will be the mechanical property.[37] In the present study, all blend systems are showing positive deviation from the line of additivity drawn between the control polymers (synergistic effect) in tensile strength and elongation at break versus composition plot. These results back up the claim of compatibilization between the two polymers in different compositions.

Morphology Studies

Morphology of all the five blend systems is studied by etching out the EMA part effectively. From the Figure 11, it can be observed that all blends are showing two phase morphology. This is the clear evidence that blends are not completely miscible with each other. However, the extracted phase which is in the form of dark cavities is sufficiently finer in size and well

dispersed as evident from the figure. It is also found that the boundaries of the cavities are vague which indicates the presence of interfacial adhesion between the CPE and EMA phase and hence proofs for their compatibilization. Moreover, the studied blend morphology is composition dependent. The particle size of dispersed EMA phase increased with increasing EMA content. This is because high concentration of dispersed phase favors coalescence of particles. Thus, in case of blends with higher EMA concentration in Figure 11(d,e) an uneven morphology with larger extracted phase is observed.[10] This composition dependent morphology influences their mechanical property and thereby C60E40 with finer domain size showed higher mechanical property than C50E50 with coarser domain size.

CONCLUSION

A systematic study has been performed for the first time to investigate the compatibility of CPE/EMA blends and their mechanical properties were also studied to analyze the effect of blend compatibility. The DSC and DMA studies of all blends show only single glass transition temperature which lies in between the T_g of control polymers. Also, the T_gs obtained from DSC measurement well fits with Couchman–Karasz equation. Moreover, appearance of all T_gs of blends obtained from both DSC and DMA are above the line of mixing rule between the control polymers. FTIR spectroscopic studies indicate presence of specific interaction between EMA and CPE due to shifting of characteristic C—Cl stretching peak of CPE and carbonyl stretching peak of EMA to lower wave number. All blends show tensile strength, elongation at break, hardness, and modulus above the line of additivity which also supports technological compatibility between the two polymers. Appearance of two phase morphology with obscure boundaries of cavities of extracted EMA phase, as observed from SEM images indicates that prepared blends are not completely miscible but compatible. From all these points, it can be concluded that CPE and EMA are technologically well compatible with each other and thus prepared blends may have potential application where the oil resistance, flame resistance, low temperature flexibility, and mechanical properties are necessary. Hence it is also expected that EMA can partially replace CPE in the field of electrical cable applications where the adverse effect of produced toxic gas by CPE on catching fire can be reduced.

REFERENCES

1. Varghese, H.; Bhagawan, S. S.; Thomas, S. *J. Appl. Polym. Sci.* **1999**, *71*, 2335.
2. Wang, L.; Zhang, Z.; Chen, H.; Zhang, S.; Xiong, C. *J. Polym. Res.* **2010**, *17*, 77.
3. Roland, C. M.; Ngai, K. L. *Macromolecules* **1991**, *24*, 2261.
4. Gomez, C. M.; Bucknall, C. B. *Polymer* **1993**, *34*, 2111.
5. Kuo, S. W.; Chang, F. C. *Macromol. Chem. Phys.* **2001**, *202*, 3112.
6. Whiteley, M. J.; Pan, W. P. *Thermochim. Acta* **1990**, *166*, 27.
7. Sirisinha, C.; Saeoui, P.; Guaysomboon, J. *J. Appl. Polym. Sci.* **2003**, *90*, 4038.
8. Ogoe, S. A.; Burns, T. D. (The Dow Chemical Co.). US Patent 5,457,146, October 10, 1995.
9. Chen, C. H.; Wesson, R. D.; Collier, J. R.; Lo, Y. W. *J. Appl. Polym. Sci.* **1995**, *58*, 1087.
10. Zhang, Z. X.; Chen, C. H.; Gao, X. W.; Kim, J. K.; Xin, Z. X. *J. Appl. Polym. Sci.* **2011**, *120*, 1180.
11. Feller, J. F.; Linossier, I.; Pimbert, S.; Levesque, G. *J. Appl. Polym. Sci.* **2001**, *79*, 779.
12. Margaritis, A. G.; Kallitsis, J. K.; Kalfoglou, N. K. *Polymer* **1987**, *28*, 2122.
13. Parmer, J. F.; Dickinson, L. C.; Chien, J. C. W.; Porter, R. S. *Macromolecules* **1989**, *22*, 1078.
14. Borah, J.; Chaki, T. *J. Polym. Res.* **2011**, *18*, 569.
15. Nishi, T.; Wang, T. *Macromolecules* **1975**, *8*, 909.
16. Cortazar, M.; Calahorra, M.; Guzman, G. *Eur. Polym. J.* **1982**, *18*, 165.
17. Couchman, P. R. *Macromolecules* **1978**, *11*, 1156.
18. Song, M.; Hammiche, A.; Pollock, H. M.; Hourston, D. J.; Reading, M. *Polymer* **1995**, *36*, 3313.
19. Paul, D. R.; Barlow, J. W. *Polymer* **1984**, *25*, 487.
20. Couchman, P. R.; Karasz, F. E. *Macromolecules* **1978**, *11*, 117.
21. Pochan, J. M.; Beatty, C. L.; Pochan, D. F. *Polymer* **1979**, *20*, 879.
22. Gordon, M.; Taylor, J. S. *J. Appl. Chem.* **1952**, *2*, 493.
23. Wood, L. A. *J. Appl. Polym. Sci.* **1958**, *28*, 319.
24. Xing, P.; Dong, L.; An, Y.; Feng, Z.; Avella, M.; Martuscelli, E. *Macromolecules* **1997**, *30*, 2726.
25. Kundu, P. P.; Tripathy, D. K.; Banerjee, S. *Polymer* **1996**, *37*, 2423.
26. Santra, R. N.; Roy, S.; Bhowmick, A. K.; Nando, G. B. *Polym. Eng. Sci.* **1993**, *33*, 1352.
27. Sirisinha, C.; Sae-Oui, P.; Guaysomboon, J. *J. Appl. Polym. Sci.* **2002**, *84*, 22.
28. Mohamad, Z.; Ismail, H.; Thevy, R. C. *J. Appl. Polym. Sci.* **2006**, *99*, 1504.
29. Radhakrishnan, C. K.; Kumari, P.; Sujith, A.; Unnikrishnan, G. *J. Polym. Res.* **2008**, *15*, 161.
30. O'Keefe, J. F. Identification of polymers by IR spectroscopy. Available: http://www.thefreelibrary.com/Identification of polymers by IR spectroscopy.-a0119376722. (accessed October 16, 2013).
31. Fekete, E.; Földes, E.; Pukánszky, B. *Eur. Polym. J.* **2005**, *41*, 727.
32. Aouachria, K.; Belhaneche-Bensemra, N. *Polym. Test.* **2006**, *25*, 1101.
33. Coleman, M. M.; Moskala, E. J.; Painter, P. C.; Walsh, D. J.; Rostami, S. *Polymer* **1983**, *24*, 1410.
34. Chakrabarti, R.; Das, M.; Chakraborty, D. *J. Appl. Polym. Sci.* **2004**, *93*, 2721.
35. Jose, S.; Aprem, A. S.; Francis, B.; Chandy, M. C.; Werner, P.; Alstaedt, V.; Thomas, S. *Eur. Polym. J.* **2004**, *40*, 2105.
36. Barentsen, W. M.; Heikens, D. *Polymer* **1973**, *14*, 579.
37. Faker, M.; Razavi Aghjeh, M. K.; Ghaffari, M.; Seyyedi, S. A. *Eur. Polym. J.* **2008**, *44*, 1834.